 doi:10.20944/preprints201810.0246.v1

Article

Preparation of PdO doped on bentonite as catalyst for Friedel-Craft acylation reaction of aromatic compounds and the investigation of the reaction mechanism

Yehezkiel Steven Kurniawan[1], Arif Cahyo Imawan[1,2], Yoeretisa Miggia Stansyah[1], Tutik Dwi Wahyuningsih[1,*]

[1] Department of Chemistry, Faculty of Mathematics and Natural Sciences, Universitas Gadjah Mada, Sekip Utara, Yogyakarta 55281, Indonesia
[2] Graduate Institute of Applied Science and Technology, National Taiwan University of Science and Technology, Keelung Rd. No. 43, Taipei 10607, Taiwan
* Correspondence: tutikdw@ugm.ac.id; Tel.: +62-818-467-863

Abstract: Catalyst material plays a pivotal role in the pharmaceutical industry process. Among them, Friedel-Craft acylation reaction is a well-known reaction to synthesis acetophenone derivatives. However, Friedel-Craft acylation mostly used acetyl chloride as starting material with Lewis acid as homogeneous catalyst, which is nonenvironmental friendly process. In this work, a simple and efficient Friedel-Craft acylation reaction is reported by using the palladium oxide doped on activated bentonite (PdOAB) as the heterogeneous catalyst. The PdOAB catalyst material was characterized with scanning electron microscopy-energy dispersive X-ray (SEM-EDX), nitrogen isotherm adsorption, Fourier transform infrared (FTIR), X-ray powder diffraction (XRD), and thermogravimetric-differential thermal analysis (TG-DTA). The acetophenone derivatives with R = -H, -Cl, -CH_3, -OCH_3, -OH and -NH_2 at para position were successfully synthesized from its corresponding aromatic compounds with glacial acetic acid in 86.6, 7.9, 91.7, 86.6, 82.7, and 78.9% yield, respectively. Therefore, a green method was established because the byproduct is water and the catalyst material can be recovered. Furthermore, the substituent (σ) constants were obtained by using Hammet equation, and the catalysis mechanism has been proposed.

Keywords: palladium oxide; bentonite; Friedel-Craft; acetophenone; catalyst.

1. Introduction

Acetophenone is an organic compound which is consist of benzene bearing the acyl group moiety [1]. Acetophenone and its derivatives were widely applied as anti-tumor [2], anti-inflammatory [3], and anti-fungal [4] agents. Furthermore, they are used in organic synthesis process of some bioactive compound, such as benzyl alcohol [5, 6], chalcone [7], benzophenone [8], pyrazoline [9], and *p*-quinol cochinchinenone [10]. Because of their important bioactivity, the demand of acetophenone derivatives is keep increasing by years. Acetophenone derivatives were mostly prepared by using Friedel-Craft acylation [11] and the oxidation of ethylbenzene [12, 13] or 1-phenylethanol [14]. Among them, Friedel-Craft acylation is a simple organic reaction between aromatic compound with acetyl chloride in the presence of homogeneous $AlCl_3$ or $FeCl_3$ as Lewis acid catalyst. This conventional reaction is a nonenvironmental friendly process because the hydrochloric acid is formed as the byproduct and the catalyst materials are hygroscopic [11].

Many researchers tried to find a green and simple method for Friedel-Craft acylation reaction. Wei et al. reported that acetyl chloride could be replaced with acetic anhydride to suppress the

 doi:10.20944/preprints201810.0246.v1

halogen waste [15]. Nakajima et al. reported that glacial acetic acid could be used and yielding higher atom economy compared with acetic anhydride [16]. However, only few reports were found for this method probably due to a narrow suitability for organic compounds and some disadvantages, such as low yield and long reaction time due to the less reactivity of acetic acid. Therefore, it is necessary to develop a green and convenient synthesis method of acetophenone derivatives [17].

Nowadays, palladium materials attract many attentions due to its high catalyst performance and wide applicability. Many novel organic reactions were developed well in a quantitative yield, such as Suzuki-Miyaura cross-coupling [18], Sonogoshira coupling [19], Buchwald-Hartwig amination [20], Heck-Matsuda reaction [21], and so on. Some stereoselective reactions were also reported by using palladium catalyst [22]. However, palladium catalysts are expensive, and thus their application is being limited [23].

Bentonite is a low-cost material due to abundantly available in the nature. Bentonite, an aluminosilicate material, constructs of an octahedral alumina layer and two tetrahedral silica layers with Brønsted and Lewis acid sites. Miranda et al. and Salmón et al. reported that bentonite materials was able to catalyzed electrophilic-substitution reaction through its Lewis acid site [24, 25]. In our previous studies, catalyst materials based on bentonite were prepared and exhibited an excellent ability and also a high efficiency for esterification [26], acetalization [27] and ketalization [28] reactions. Moreover, bentonite framework provides a unique three-dimensional structure that contributes to the high selectivity of the reaction product [29]. A combination between palladium and bentonite materials as catalyst could enhance the efficiency of the Friedel-Craft acylation reaction.

In the present work, three types of materials were prepared, i.e. natural bentonite (NB), activated bentonite (AB), and palladium oxide doped onto activated bentonite (PdOAB) and used as heterogeneous catalyst for Friedel-Craft acylation reaction. The activation of NB was carried out by using sulfuric acid at 80 °C for 3 h and then the palladium(II) ions were doped onto AB to obtain PdOAB. All catalyst materials were applied to find an optimum condition to prepare some acetophenone derivatives with the R = -H, -Cl, -CH_3, -OCH_3, -OH and -NH_2 at the para position. The reaction equation was shown in Figure 1. The catalytic activity was evaluated by a comparison with NB and AB in lieu of the PdOAB. In our previous work, an unsteady state diffusion model was proposed and applied to understand the slow release mechanism of urea and also predicted the urea interaction onto the host material as well [30]. In this work, another mathematical model, that was Hammet equation was used to analyze the effect of the various aromatic compounds with PdOAB catalyst material to the Friedel-Craft acylation reaction. Even though the Hammet analysis in the organic synthesis reactions was rarely reported, it is critical to understand the physical organic aspect to optimize the reaction process as well as to propose the catalysis mechanism.

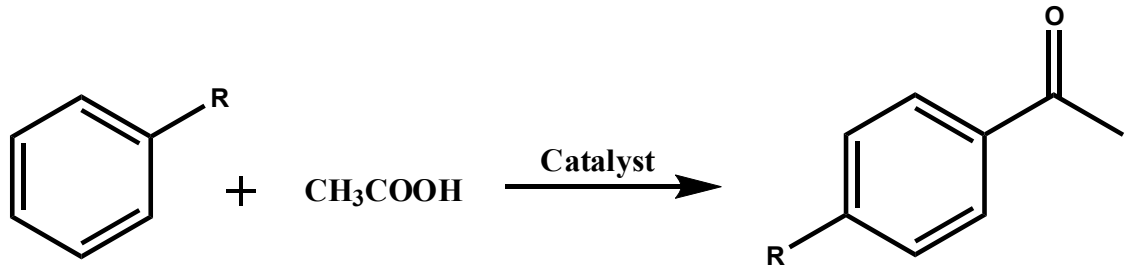

Figure 1. The synthesis of acetophenone derivatives

2. Results and Discussion

2.1. Preparation of AB and PdOAB materials

The AB material was prepared through the activation of NB by using sulfuric acid. The common metal ions (*e.g.* sodium, potassium, iron, calcium and aluminium [32]) in the bentonite interlayer were

 doi:10.20944/preprints201810.0246.v1

exhanged with protons from the sulfuric acid solution to yield AB material. By using sulfuric acid, the metal ions were exchanged with protons. Afterwards, the palladium(II) ions replaced the protons and PdO was doped onto the surface of the AB material when the pH was increased by using ammonia solution.

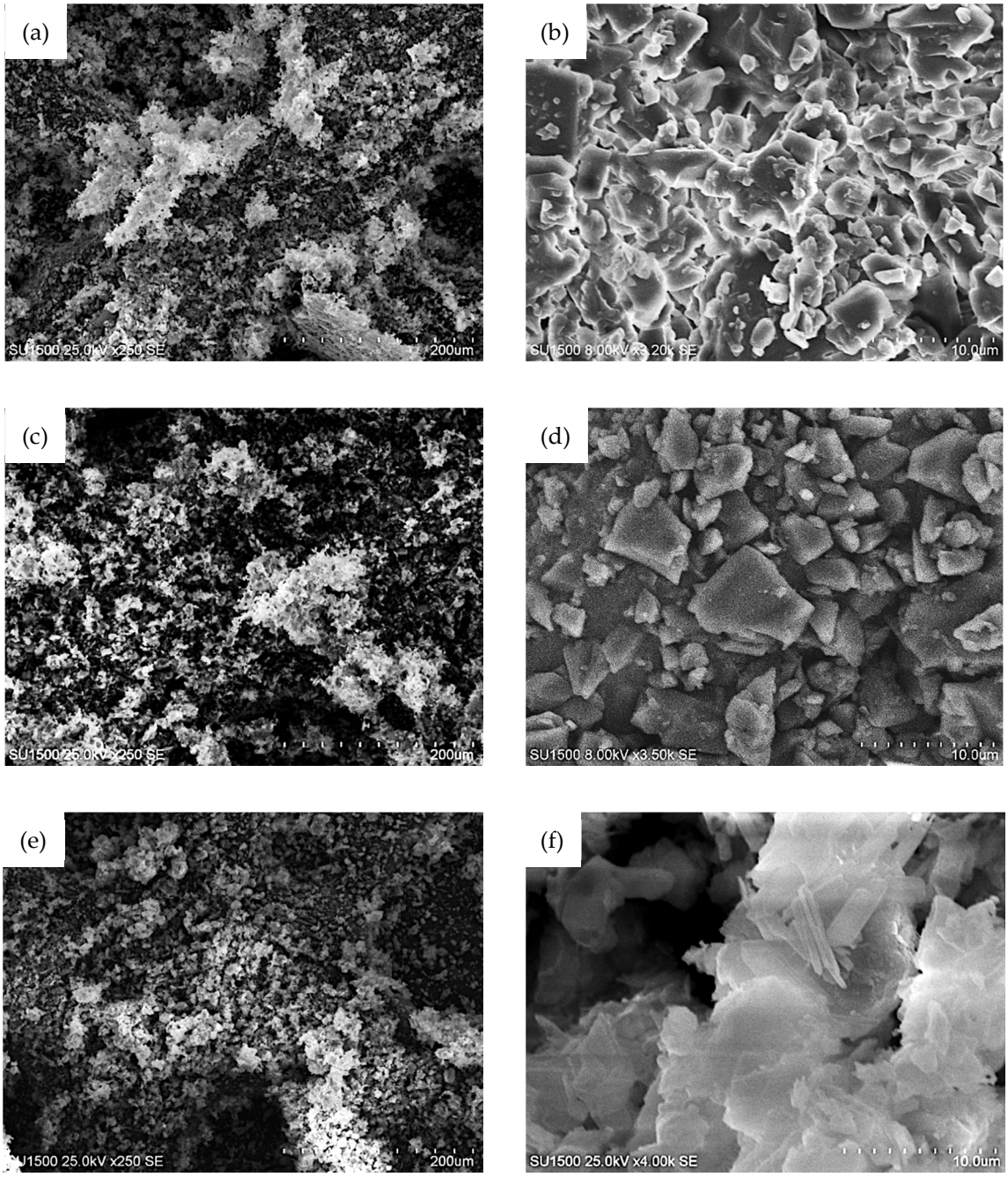

Figure 2. SEM morphology of natural bentonite (a and b) activated bentonite (c and d) and PdO doped on bentonite (e and f)

The morphology of the NB, AB and PdOAB materials were photographed by SEM and shown in Figure 2. It showed that the morphology of AB was similar with NB but different from PdOAB. The PdOAB material was agglomerated probably due to the strong ionic interaction between PdO with the surface of the AB. From the Figure 2(f), the presence of tetragonal particles located on the bentonite surface, confirmed that the PdO was sucessfully doped on the surface of the bentonite. The

Preprints (www.preprints.org) | NOT PEER-REVIEWED | Posted: 12 October 2018 doi:10.20944/preprints201810.0246.v1

surface area and the total pore volume of the material were obtained from the nitrogen isotherm adsorption experiment. It showed that after doping of PdO on the AB material, the surface area of the material decreased from 6.277 to 2.057 m^2 g^{-1}, and the total pore volume decreased from 12.04 to 8.688 mm^3 g^{-1}. The decrease of the surface area and total pore volume occurred caused by the agglomeration of the material after PdO doping. To quantify the palladium percentage in the PdOAB material, the EDX analysis was recorded in triplicate for each sample. From the Table 1, the presence of the metal cations, such as iron, sodium, calcium and aluminium were not detected, except a small amount of potassium and titanium. However, after PdO doping, both remains cation were replaced with palladium. The average mass percentage of the palladium in the PdOAB material was 3.87%.

Table 1. Elemental composition of AB and PdOAB materials

Elements	Mass percentage (%)	
	AB	PdOAB
Oxygen	49.48	43.99
Aluminium	9.36	9.34
Silicon	38.81	42.8
Titanium	1.92	0.00
Potassium	0.44	0.00
Palladium	0.00	3.87

To confirm the palladium species and crystal structure, the X-ray diffractogram were measured and shown in Figure 3. The peak d_{001} at $2\theta = 10°$ of the AB (Figure 3(b)) was decreased compared with NB (Figure 3(a)). It confirms that the amount of the metal ions on the bentonite interlayer was decreased and showed that the activation of NB was successfully conducted. Furthermore, new peaks were appeared at 2θ around 29, 33 and 41, in which correspond to the PdO peak with tetragonal crystal system (JCPDS 00-043-1024) and confirmed that the doping process of PdO on the AB material took place. It was also confirmed from the Figure 2d, that the tetragonal particles on the bentonite surface were PdO.

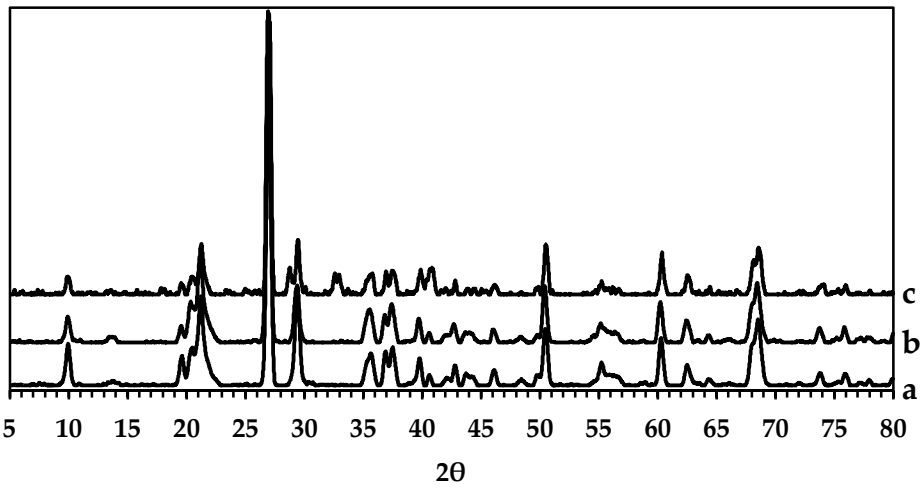

Figure 3. Diffractogram of a) NB, b) AB and c) PdOAB materials

The FTIR spectra of NB, AB and PdOAB were shown in Figure 4. The Si-O-Si peak at 939 cm^{-1} decreased due to the activation process of NB. On the other hand, the TG-DTA graph of the PdOAB

Preprints (www.preprints.org) | NOT PEER-REVIEWED | Posted: 12 October 2018 doi:10.20944/preprints201810.0246.v1

material is shown in Figure 5. The PdOAB material underwent endothermic process at 225 and 300 °C, however the mass loss percentage was less than 10%. It showed that the PdOAB material has a good thermal stability even at 850 °C, thus it can be applied as catalyst material at that temperature range.

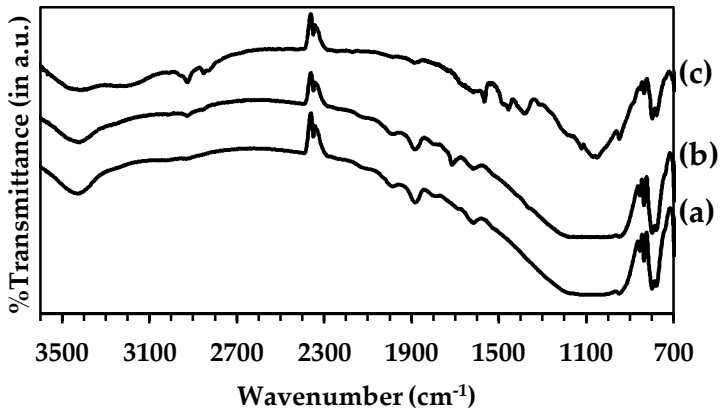

Figure 4. FTIR spectra of a) NB, b) AB and c) PdOAB materials

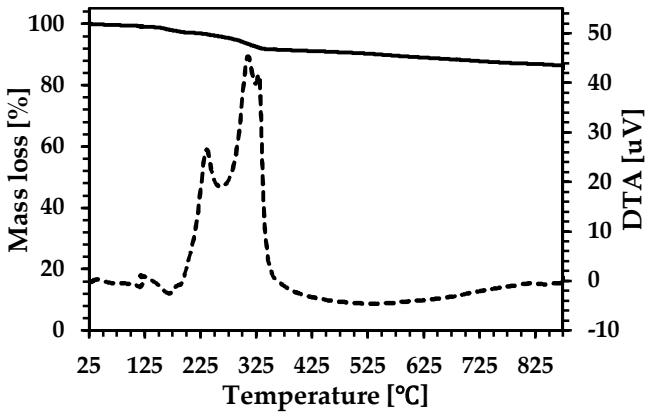

Figure 5. TG-DTA graph of the PdOAB material (Solid line: TG; Dotted line: DTA)

2.2. The effect of catalyst mass and reaction time span towards the yield of the acetophenone products

In this work, the acylation reaction of the aromatic compounds gave the para subtituted acetophenone as the major product, while the ortho product was not regarded. Figure 6 showed the effect of the catalyst mass towards the yield of the acetophenone product at 5 h reaction time. Overall, the acetophenone derivatives produced shot up with the increase of the catalyst mass. However, the yield of some acetophenone derivatives decreased by the increase of the catalyst mass due to the adsorption process on the catalyst material. Compared to the uncatalyzed reaction (m = 0.00 mg), NB was able to increase the products yield until 20% (Figure 6(a)) because of the acid sites of the NB catalyst were occupied with other metal ions, such as sodium, potassium, calcium and so on. Therefore just a few amounts of aromatic compounds were activated on the catalytic sites.

Preprints (www.preprints.org) | NOT PEER-REVIEWED | Posted: 12 October 2018 doi:10.20944/preprints201810.0246.v1

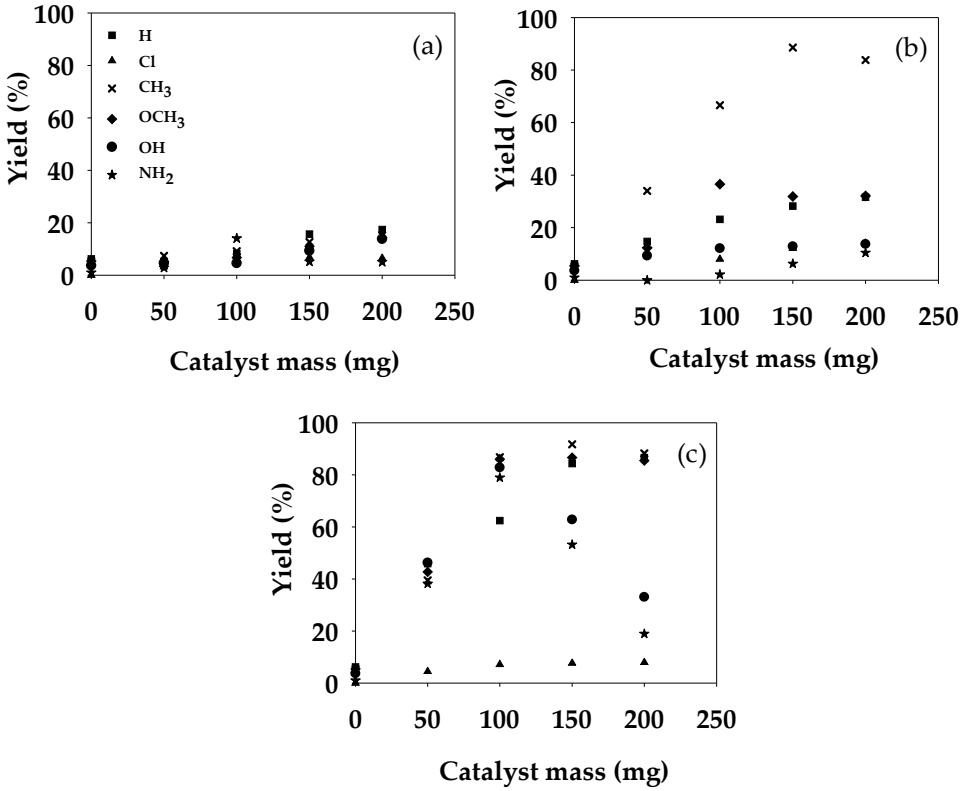

Figure 6. Dependency profile from the synthesis of acetophenone derivatives with the mass of (a) NB, (b) AB and (c) PdOAB catalyst materials

Figure 6(b) showed that the AB catalyst was more effective than NB catalyst due to the activation process. The yields of the products reached the equilibrium state when 200 mg catalyst was employed. However, the yield of the products (except 4-methylacetophenone) were not satisfied enough. The yield of the products were affected by the kind of R substituent. The electron donor substituents, such as methyl, methoxy and hydroxy, tend to increase the yield because the aromatic ring became more active to react. Even though the amino group is an electron donor substituent, the yield of the 4-aminoacetophenone reached 10.41% only by using 200 mg AB catalyst. It occurred because the amino substituent acted as a base, therefore, it was very easy to interact with the acid sites of AB catalyst and became protonated. Likewise, electron withdrawing group, i.e. chloride gave a low yield.

Figure 6(c) showed that the PdOAB can enhance the reaction yields, therefore this material was the most efficient catalyst compared to NB or AB. The doped PdO onto the surface of the activated bentonite could activate the the reactant via Lewis acid-base interaction, and consequently, the yield of the products remarkably increased. It was found that 150 mg of PdOAB catalyst was enough to reach the equilibrium state, however, the yield of the 4-hydroxyacetophenone and 4-aminoacetophenone were drastically reduced when the catalyst mas was over than 150 mg. It was caused by the interaction between palladium metal ion and the hydroxy or amino groups as the ligand.

The catalyst efficiency was in a good correlation with the acid sites of each catalyst. Brønsted and Lewis acid sites were determined from the vapour adsorption of ammonia and pyridine on the

 doi:10.20944/preprints201810.0246.v1

catalyst surface. The Brønsted acid sites on the NB, AB and PdOAB materials were 2.89, 8.66 and 3.51 mmol g^{-1}, respectively, while Lewis acid sites were 4.08, 3.29 and 7.16 mmol g^{-1}, respectively. It was confirmed that the catalytic efficiency of AB is better than NB due to a high Brønsted acid sites, because the Friedel-Craft acylation required Brønsted acid sites for the formation of the acylium ion as the intermediate [15]. Even though, the Brønsted acid sites of the PdOAB decreased compared with AB catalyst, however, the catalytic activity was better. It was due to the presence of a higher Lewis acid sites that could stabilize the reaction intermediates [33-35].

The reaction time of the Friedel-Craft acylation was investigated to find the optimum reaction time for each catalyst on each optimum catalyst mass. Figure 7(a) showed that all of the reactions have not reached the equilibrium even in 6 h. Moreover, without any catalyst, the yield of the products was very low, that was not more than 8%. Figure 7(b)-(d) shows the effect of the catalyst materials on the yield of the products. Overall, the yield of the products increased compared to the uncatalyzed reaction. It meant that the bentonite materials can be used as the catalyst for the Friedel-Craft acylation reaction due to the presence of the acid catalytic sites. Since the AB had more active acid sites than NB, the catalytic activity of the AB was better than NB. Figure 7(c) showed that the reactions between 4-methoxybenzene and acetic acid glacial reached the equilibrium state after 5 h reaction time, however, it was reduced to 4 h reaction time by using PdOAB catalyst material as shown in Figure 7(d). It was occurred due to the additional catalytic sites from the PdOAB material.

The required time to reach the reaction equilibrium state was determined from the plot between reaction rate and reaction time as shown in Figure S1. The equlibrium state reached when the reaction rate ($\frac{dr}{dt}$) reached the zero value. Figure S1 showed that PdOAB remarkably enhanced the initial reaction rate 1.67-16.89 times faster that AB catalyst, therefore the time reaction of the the reaction catalyzed by PdOAB was shorten. Table 2 shows the optimum condition for Friedel-Craft acylation of the benzene derivatives over the varied substituents. The reaction order and rate constant were calculated from equation (3) and shown in Table 3. Even though the reaction order and rate constant for 4-chlorobenzene in not satisfied, other Friedel-Craft reactions were described well. The reaction order was around 1.00 for benzene derivatives with R = -H, $-CH_3$, and $-OCH_3$ substituents, showing that the unimolecular reactions were occurred. On the other hand, the bimolecular reactions were found for the acylation of benzene derivatives with -OH and $-NH_2$ groups.

The PdOAB catalyst material was the best among the others, except for 4-chloroacetophenone that might be due to the strong electronic interaction between palladium as the soft acid and/or Lewis acid sites with chloride as the soft base [36]. However, further investigation is required to understand the interaction between chloro substituent with PdOAB catalyst material in details. The results demonstrating that PdOAB catalyst was more efficient than either AB and NB catalyst materials.

Preprints (www.preprints.org) | NOT PEER-REVIEWED | Posted: 12 October 2018 doi:10.20944/preprints201810.0246.v1

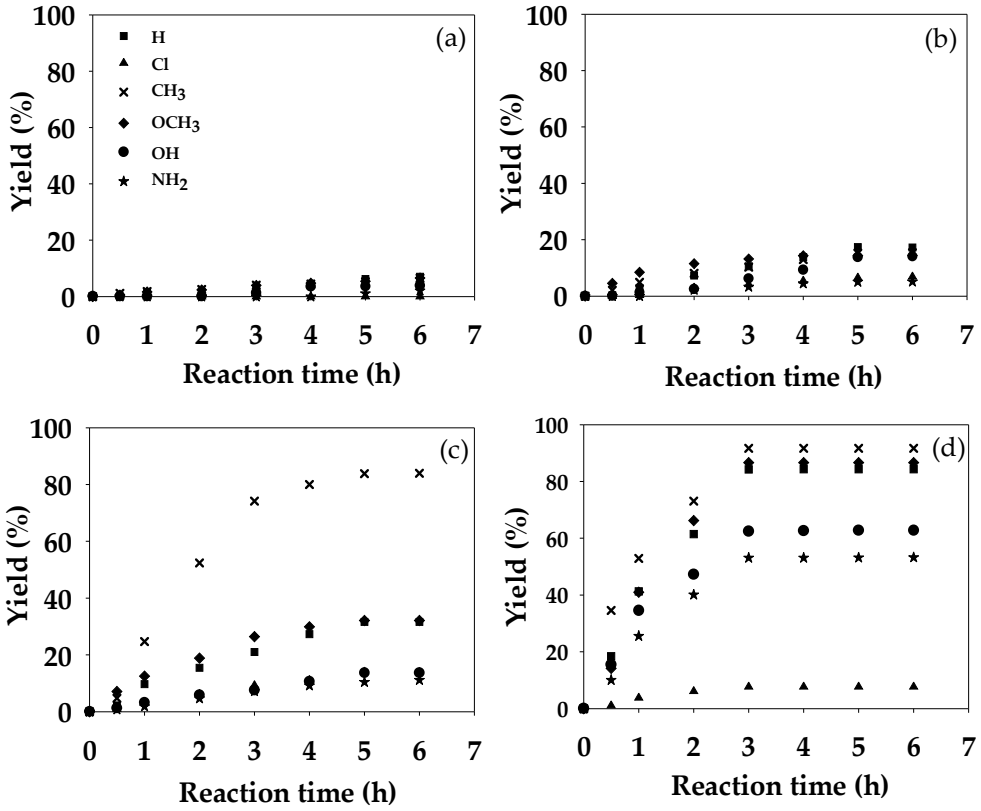

Figure 7. Reaction time dependency profile from the synthesis of acetophenone derivatives without any catalyst (a) and with (b) NB, (c) AB and (d) PdOAB catalyst materials

186

187 **Table 2.** The optimum reaction condition for the Friedel-Craft acylation

R	Catalyst	Catalyst mass (mg)	Reaction time (h)	Yield (%)
H	PdOAB	150	5	84.24
Cl	AB	200	5	14.01
CH_3	PdOAB	150	4	91.65
OCH_3	PdOAB	150	5	86.63
OH	PdOAB	150	4	62.42
NH_2	PdOAB	150	5	53.07

188

189 **Table 3.** The kinetic parameter of the Friedel-Craft acylation catalyzed by PdOAB

R	R^2	M	k'
H	0.992	0.85	0.735
Cl	0.888	18.89	$2.679 \cdot 10^{-25}$
CH_3	0.998	1.11	0.603
OCH_3	0.997	0.72	1.069
OH	0.966	2.12	0.018
NH_2	0.970	2.11	0.012

190

Preprints (www.preprints.org) | NOT PEER-REVIEWED | Posted: 12 October 2018 doi:10.20944/preprints201810.0246.v1

2.3. Reusability of PdOAB material

To evaluate the reusability of the PdOAB catalyst material, the optimum condition for 4-methoxyacetophenone was selected. The catalyst material was recovered after reaction by filtration and then dried and also reused as the catalyst. The reaction yield decreased cycle by cycle of the reaction and reached constant at 71.4% yield in the third cycle, as shown in Table 4. It was caused by the palladium ions were leaked from the PdOAB material to the acidic solution. It showed that the palladium(II) plays a pivotal role in the reaction mechanism. The percentage of the eluted palladium was calculated from the aqueous phase by using FAAS in a comparison with the initial palladium concentration in the material (3.87% weight) from the EDX analysis (Table 1). Even though the palladium was leaked, the catalyst activity was still high enough, therefore it showed that the heterogeneous PdOAB catalyst material was an efficient material that could be easily recovered and reused by a simple filtration process.

Table 4. PdOAB catalyst recycling investigation

Cycle	Eluted Palladium (%)	Reaction yield (%)
1	8.09	86.6
2	10.33	75.2
3	10.65	71.4
4	10.65	71.4

2.4. Hammet analysis of the synthesis of acetophenone reaction

To understand the catalytic mechanism, the Hammet analysis was carried out. Based on the equation (4), the σ values for each substituent (Table 5) were predicted with an assumption that ρ was 1.00. If the σ value was negative, the substituent can pull the electron density of the aromatic ring to the para position, therefore its ability to act as nucleophile was reduced. The σ value for chloro substituent was not satisfied due to its poor yield and its catalytic inhibition to PdOAB Lewis sites. The amino and hydroxyl groups, which usually had positive σ value [31], showed negative σ values. It caused by whether strong hydrogen bonding interaction with acid sites of the catalyst or the protonation of the hydroxyl and amino functional groups in the acidic condition to form $-OH_2^+$ and $-NH_3^+$, respectively. Therefore the electron density was getting further from the para position. The methyl group is an activator substituent, however, the σ values of the hydrogen and the methyl group were similar. Methoxy group is one of the strong activator substituent, therefore the σ value of methoxy group was positive as expected.

Table 5. The σ constant for each substituent

R	σ
H	0.00
CH_3	-0.09
OCH_3	0.16
OH	-1.62
NH_2	-1.78

3.5. Proposed mechanism of the catalyzed Friedel-Craft acylation reaction with PdOAB material

Preprints (www.preprints.org) | NOT PEER-REVIEWED | Posted: 12 October 2018 doi:10.20944/preprints201810.0246.v1

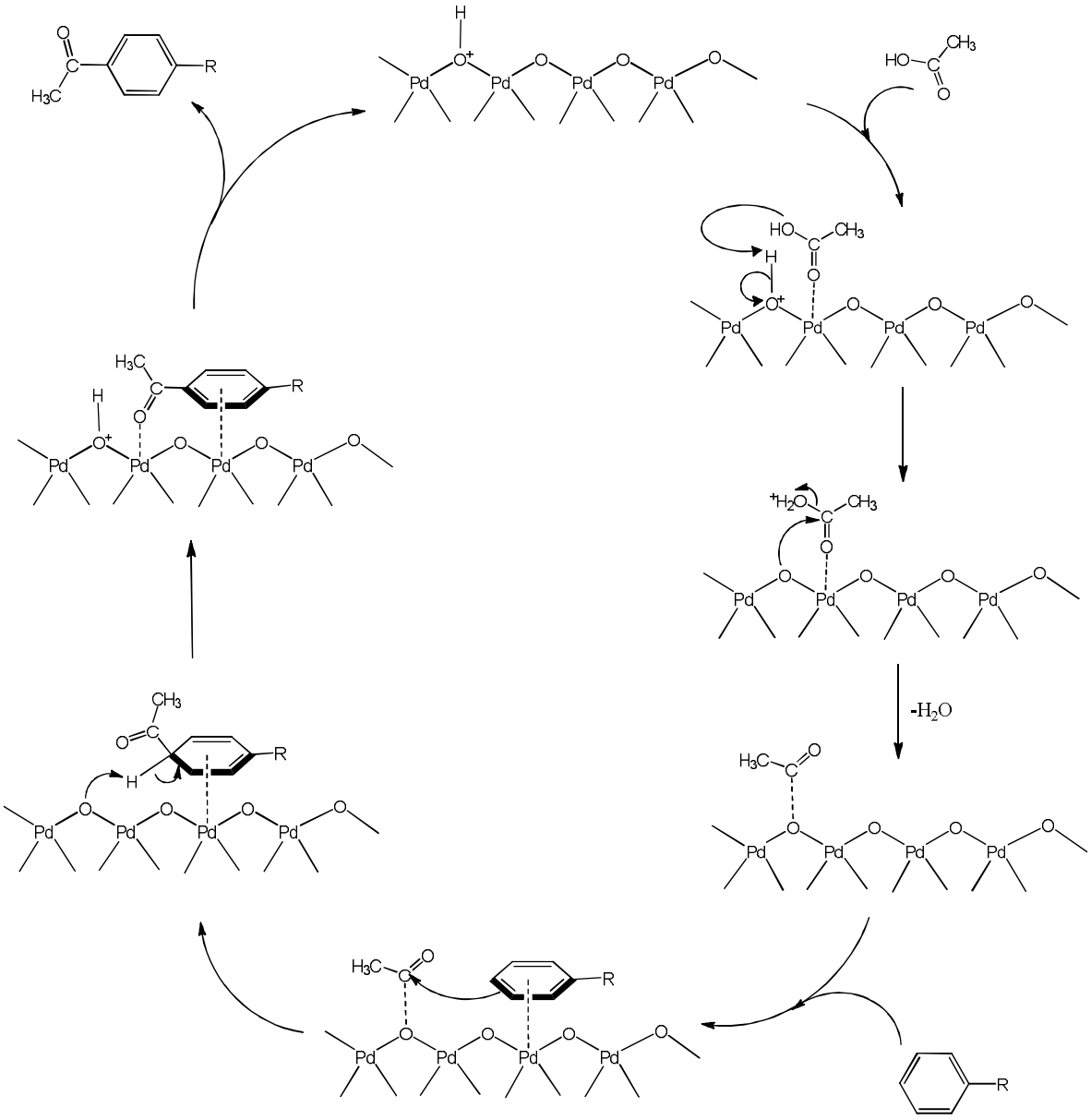

Figure 8. Plausible reaction mechanism of the Friedel-Craft acylation involving the acid site of the PdOAB catalyst

The catalyzed Friedel-Craft reaction mechanism was predicted based on the physicochemical properties of the PdOAB material and its catalytic activity. From the SEM (Figure 2(f)) and XRD (Figure 3(c)) results, the tetragonal palladium oxide was located on the surface of the material, therefore increased the Lewis acid sites of the catalyst material. Many researchers reported that the catalyzed acylation reaction mechanism strongly depended on the acidity properties of the materials [15, 35, 37]. The AB material had higher Brønsted acid sites, therefore it showed a higher catalytic activity than the NB material and gave a higher yield toward Friedel-Craft acylation reaction. However, the catalytic activity of the PdOAB material was the highest, even though it had lower Brønsted acid sites but higher Lewis acid sites compared with AB. It meant that both acid sites were important for the reaction catalysis mechanism. However, Lewis acid sites seem to play a pivotal role on the PdOAB catalytic reaction mechanism. The first reason is the yield of the reaction depends on the palladium concentration in the PdOAB material (Table 4), while the second is the catalytic activity of the PdOAB for 4-chlorobenzene was lower than AB (Figure 7) due to the suitable interaction

 doi:10.20944/preprints201810.0246.v1

between the chloro substituent as soft base and the palladium(II) ion as soft acid. From these results, the reaction mechanism with PdOAB catalyst was proposed and shown in Figure 8.

At first, the acetic acid was adsorbed on the Lewis acid sites of the palladium ion. Then the hydroxyl group of the acetic acid was protonated and generated the acylium ion and water as the byproduct. Afterwards, the aromatic compound was adsorped on the catalyst surface through the π-π interaction between aromatic ring and palladium ion as well as the dipole interaction between palladium ion and the polar R groups (R = Cl, OH, OCH_3 and NH_2). Because of both interactions and the steric hindrance, the acylation of the aromatic compound selectively occurred on the para position. This step seems to be the rate-determining step, because the yield of the product was affected by the kind of R substituent as well as the catalyst amount. For R substituent with a positive σ value (R = CH_3), the intermediate was stabilized and consequently, the yield of the reaction was remarkably enhanced. For the R substituent with a value near to zero (R = H and OCH_3), the intermediate was not strongly adsorped on the PdOAB surface, therefore, the electron density of the aromatic ring was enough to react with the acylium ion. However, the R substituent with a negative σ value, such as OH and NH_2 groups, the aromatic compound was strongly adsorped due to its interaction with palladium ion, therefore the electron density of the aromatic ring was not strong enough to attack the acylium ion. It was also confirmed in Figure 6(c), in which the yield of the product was decreased if the catalyst mass was more than 100 mg. Finally, the acetophenone derivative product was desorped and the catalyst active site was regenerated. This reaction mechanism was in agreement with the other result. Frouri *et al.* reported that furfural acylation was facilitated by the additional Lewis sites from the alumunium(III) on the hydroxyide fluoride catalyst [35].

3. Conclusions

The activation of the bentonite material and PdO doping on the activated bentonite have been conducted to obtain AB and PdOAB catalyst materials. The prepared catalyst materials were characterized by SEM, EDX, FTIR, XRD and TG-DTA analysis. These catalysts (i.e. NB, AB and PdOAB) were applied in the synthesis of the several acetophenone derivatives via Friedel-Craft acylation reaction. The kinetic analysis of these catalytic reactions has been carried out and resulting that the PdOAB catalyst was the most efficient catalyst compared to NB and AB catalysts. The Friedel-Craft acylation reactions catalyzed by PdOAB were unimolecular or bimolecular reaction depend on the substituent of the reactants. The proposed mechanism of these catalytic reactions showed that the interaction of the reactant and catalyst was more dominant through Lewis acid site instead of Brønsted acid site. By employing a reusable PdOAB catalyst material for the Friedel-Craft acylation, a simple, green and efficient reaction process has been achieved.

4. Materials and Methods

4.1. Materials

Glacial acetic acid, benzene, chlorobenzene, anisole (methoxybenzene), toluene (methylbenzene), phenol (hydroxybenzene), aniline (aminobenzene), palladium(II) nitrate, anhydrous sodium sulfate, ammonia solution and chloroform were purchased from E. Merck (Germany) in analytical grade and used as it is without any further purification, while the natural bentonite was obtained from Tasikmalaya, West Java, Indonesia.

4.2. Equipments

Fourier transform infrared (FTIR) spectra of the catalyst materials and synthesized products were recorded on a Shimadzu Prestige-21 FT-IR spectrophotometer. Proton nuclear magnetic

 doi:10.20944/preprints201810.0246.v1

resonance (^{1}H-NMR) spectra were obtained in the deuterated chloroform on a JEOL-MY 500 proton NMR spectrometer. The X-Ray diffractogram of the catalyst materials was recorded on an X-Ray Diffraction (XRD) Shimadzu S-6000. The surface morphology and elemental composition of the catalyst materials were measured by using scanning electron microscope (SEM) with energy dispersive X-ray (EDX) on JEOL JSM-6510. The thermal stability of catalyst materials was evaluated by thermogravimetric-differential thermal analysis (TG-DTA) while the surface area of the catalyst materials was measured by using Brunauer-Emmett-Teller (BET) method from the nitrogen physisorption. Flame Atomic Absorption Spectroscopy (FAAS) was used to measure the palladium concentration which was released from the heterogeneous catalyst material into the solution mixture.

4.3. Bentonite activation in the acidic solution

At first, the mashed NB was filtered to 100 mesh. Then 100 g of the material was soaked in 300 mL of 1.0 mol dm^{-3} sulfuric acid and heated at 80 °C for 3 h. The mixture washed with distilled water until neutral. The residue was dried at 120 °C for 6 h and then filtered to 100 mesh. The obtained AB material was characterized by SEM-EDX, BET, FTIR, and XRD.

4.4. Preparation of PdOAB material

As much as 4.0 g of activated bentonite was added into the 20 mL of 0.1 M palladium(II) nitrate solution and stirred for 30 min. The ammonia solution (20 mL, 6.0 M) was added dropwise and the mixture was stirred overnight at room temperature. The mixture was filtered, and the residue was dried at 120 °C for 6 h and then homogenized to 100 mesh. The PdOAB material was characterized by SEM-EDX, BET, FTIR, XRD and TG-DTA.

4.5. Acetophenone synthesis

Under the nitrogen atmosphere, as much as 1.56 g (20 mmol) benzene was added into 25 mL (438 mmol, 22 equivalent) of glacial acetic acid. Then, the catalyst (NB or AB or PdOAB) was added into the solution. The mass of catalyst was varied from 0 (without catalyst); 0.05; 0.10; 0.15 and 0.20 g to find the optimum mass of each catalyst material. The mixture was refluxed for 6 h and then filtered to separate catalyst and the crude product, after that the product was extracted from crude product into the chloroform. The organic layer was washed with distilled water and dried over anhydrous sodium sulfate. The chloroform was evaporated to obtain the desired product. The other acetophenone derivatives, *i.e.* 4-chloroacetophenone, 4-methylacetophenone, 4-methoxyacetophenone, 4-hydroxyacetophenone and 4-aminoacetophenone were obtained in a similar manner as described above. Especially, additional acid hydrolysis process was required to hydrolyze the ester and amide functional groups of the intermediate to obtain the 4-hydroxyacetophenone and 4-aminoacetophenone as final products. The FTIR and 1H-NMR spectra of the obtained products were similar to the standard compounds. The reaction time was also varied from 0.5; 1; 2; 3; 4; 5 and 6 h to obtain the optimum reaction time.

Acetophenone. IUPAC name: 1-Phenylethanone. C_8H_8O. FTIR (KBr, cm^{-1}), 3089 (C-H sp^2), 2969 (C-H sp^3), 1691 (C=O), 1584 and 1450 (C=C aromatic). ^{1}H-NMR ($CDCl_3$, δ/ppm) 2.44 (s, 3H, $COCH_3$), 7.30 (t, 2H, Ar-H *meta*), 7.42 (t, 1H, Ar-H *para*), 7.84 (d, 2H, Ar-H *ortho*).

4-Chloroacetophenone. IUPAC name: 1-(4-Chlorophenyl)ethanone. C_8H_7ClO. FTIR (KBr, cm^{-1}), 3064 (C-H sp^2), 2968 (C-H sp^3), 1687 (C=O), 1589 and 1488 (C=C aromatic), 588 (C-Cl). ^{1}H-NMR ($CDCl_3$, δ/ppm) 2.67 (s, 3H, $COCH_3$), 7.41 (d, 2H, Ar-H *meta*), 7.83 (d, 2H, Ar-H *ortho*).

 doi:10.20944/preprints201810.0246.v1

4-Methylacetophenone. IUPAC name: 1-(4-Tolyl)ethanone. $C_9H_{10}O$. FTIR (KBr, υ/cm^{-1}), 3052 (C-H sp^2), 2968 (C-H sp^3), 1682 (C=O), 1574 and 1430 (C=C aromatic). ^{1}H-NMR ($CDCl_3$, δ/ppm) 2.34 (s, 3H, CH_3), 2.59 (s, 3H, $COCH_3$), 6.61 (d, 2H, Ar-H *meta*), 7.51 (d, 2H, Ar-H *ortho*).

4-Methoxyacetophenone. IUPAC name: 1-(4-Methoxyphenyl)ethanone. $C_9H_{10}O_2$. FTIR (KBr, cm^{-1}), 3000 (C-H sp^2), 2941 (C-H sp^3), 1668 (C=O), 1577 and 1445 (C=C aromatic), 1261 (C-O). ^{1}H-NMR ($CDCl_3$, δ/ppm) 2.59 (s, 3H, $COCH_3$), 3.79 (s, 3H, OCH_3), 6.77 (d, 2H, Ar-H *meta*), 7.51 (d, 2H, Ar-H *ortho*).

4-Hydroxyacetophenone. IUPAC name: 1-(4-Hydroxyphenyl)ethanone. $C_8H_8O_2$. FTIR (KBr, cm^{-1}), 3147 (O-H), 3019 (C-H sp^2), 2963 (C-H sp^3), 1588 (C=O), 1515 and 1441 (C=C aromatic), 1286 (C-O). ^{1}H-NMR ($CDCl_3$, δ/ppm) 2.61 (s, 3H, $COCH_3$), 7.06 (d, 2H, Ar-H *meta*), 7.84 (d, 2H, Ar-H *ortho*), 8.69 (s, 1H, OH).

4-Aminoacetophenone. IUPAC name: 1-(4-Aminophenyl)ethanone. C_8H_9NO. FTIR (KBr, cm^{-1}), 3396 and 3324 (H-N-H), 3064 (C-H sp^2), 2956 (C-H sp^3), 1594 (C=O), 1568 and 1439 (C=C aromatic), 1283 (C-N). ^{1}H-NMR ($CDCl_3$, δ/ppm) 2.47 (s, 3H, $COCH_3$), 4.31 (s, 2H, NH_2), 6.69 (d, 2H, Ar-H *meta*), 7.74 (d, 2H, Ar-H *ortho*).

4.6. Kinetic of the Friedel-Craft acylation catalyzed by PdOAB catalyst material

The rate equation of the Friedel-Craft acylation reaction was given by equation (1)

$$r = \frac{d[\text{product}]}{dt} = k\,[\text{benzene derivative}]^m[\text{acetic acid}]^n \quad (1)$$

where r is the reaction rate, t is the reaction time, k is the rate constant, and m and n are the reaction order towards benzene derivative and acetic acid, respectively. The reaction rate was obtained as gradient for a graph between product concentration (mmol dm^{-3}) and reaction time (h). Since the acetic acid concentration was in excess amount, the equation (1) can be simplified to equation (3), therefore m and k′ values can be obtained as slope and intercept, respectively.

$$\frac{d[\text{product}]}{dt} = k'\,[\text{benzene derivative}]^m \quad (2)$$

$$\log\left\{\frac{d[\text{product}]}{dt}\right\} = m \cdot \log[\text{benzene derivative}] + \log k' \quad (3)$$

4.7. Analysis of the substituent variations effect (σ) in the synthesis of acetophenone derivatives

The effect of the substituent variations in the synthesis of acetophenone derivatives has been analyzed by using the Hammet equation as described below [31]

$$\log\frac{k'}{k'_o} = \sigma\rho \quad (4)$$

where k'_o is the experimental rate constant of the reaction for benzene (R = -H), k′ is the experimental rate constant for benzene with other substituents, σ is the substituent constant, and ρ is the reaction constant.

Supplementary Materials: The following are available online at www.mdpi.com/xxx/s1, Figure S1: Time course dependency on the reaction rate of the Friedel-Craft acylation reaction catalyzed by NB, AB and PdOAB for (a) acetophenone, (b) 4-chloroacetophenone, (c) 4-methylacetophenone, (d) 4-methoxyacetophenone, (e) 4-hydroxyacetophenone, and (f) 4-aminoacetophenone

Author Contributions: T.D.W. and Y.S.K. conceived and designed the experiments; Y.S.K., Y.M.S. and A.C. performed the experiments; A.C. and Y.M.S. analyzed the data; A.C. contributed materials/analysis instrument; Y.S.K. and A.C. wrote the paper; all authors read and approved the final manuscript.

Funding: This research received no external funding

Acknowledgments: The authors express a gratitude to Mr Limpat Nulandaya (Pukyeong National University, South Korea) for his kind help on the XRD measurement and interpretation, as well as Mr Ilyas Taufik Abdul Aziz (Universitas Gadjah Mada) and Mr Philip Anggo Krisbiantoro (Hokkaido University, Japan) for his advice on the characterization of the materials.

Conflicts of Interest: The authors declare no conflict of interest.

References

1. Nania, S.L.; Shaw, S.K.; Structural Changes in Acetophenone Fluid Films as a Function of nano-Scale Thickness. *Langmuir* **2017**, 1-15. **Doi:** 10.1021/acs.langmuir.6b04206.
2. Morita, C.; Kobayashi, Y.; Saito, Y.; Miyake, K.; Tokuda, H.; Suzuki, N.; Ichiishi, E.; Lee, K.H.; Nakagawa-Goto, K.; Total Synthesis and in Vitro Anti-Tumor-Promoting Activities of Racemic Acetophenone Monomers from Acronychia trifoliolata. *J. Nat. Prod.* **2016**, 79, 2890-2897. Doi: 10.1021/acs.jnatprod.6b00646.
3. Sim, T.Y.; Harith, H.H.; Tham, C.L.; Hashim, N.F.M.; Shaari, K.; Sulaiman, M.R.; Israf, D.A. The protective effects of a synthetic geranyl acetophenone in a cellular model of tnf-α-induced pulmonary epithelial barrier dysfunction. *Molecules* **2018**, 23, 1355. Doi: 10.3390/molecules23061355
4. Yoon, M.Y.; Choi, N.H.; Min, B.S.; Choi, G.J.; Choi, Y.H.; Jang, K.S.; Han, S.S.; Cha, B.; Kim, J.C.; Potent in Vivo Antifungal Activity against Powdery Mildews of Pregnane Glycosides from the Roots of Cynanchum wilfordii. *J. Agric. Food Chem*. **2011** 59, 12210-12216. Doi: 10.1021/jf2039185
5. Ruelas-Leyva, J.P.; Fuentes, G.A. Chiral catalyst deactivation during the asymmetric hydrogenation of acetophenone. *Catalysts* **2017**, 7, 1-11. Doi: 10.3390/catal7070193
6. Dong, F.; Zhou, Y.; Zeng, L.; Watanabe, N.; Su, X.; Yang, Z. Optimization of the Production of 1-Phenylethanol Using Enzymes from Flowers of Tea (Camellia sinensis) Plants. *Molecules* **2017**, 22, 131. Doi: 10.3390/molecules22010131.
7. Feng, L.; Maddox, M.M.; Alam, M.Z.; Tsutsumi, L.S.; Narula, G.; Bruhn, D.F.; Wu, X.; Sandhaus, S.; Lee, R.B.; Simmons, C.J.; Tse-Dinh, Y.C.; Hurdle, J.G.; Lee, R.E.; Sun, D. Synthesis, Structure–Activity Relationship Studies, and Antibacterial Evaluation of 4-Chromanones and Chalcones, as Well as Olympicin A and Derivatives, *J. Med. Chem*., **2014**, 57, 8398-8420. Doi: 10.1021/jm500853v.
8. Wang, X.; Liu, F.D.; Tu, H.Y.; Zhang, A.D. One-Pot Synthesis of Diarylmethanones through Palladium-Catalyzed Sequential Coupling and Aerobic Oxidation of Aryl Bromides with Acetophenone as a Latent Carbonyl Donor. *J. Org. Chem*., **2014**, 79, 6554-6562. Doi: 10.1021/jo5010185.
9. Havrylyuk, D.; Zimenkovsky, B.; Vasylenko, O.; Gzella, A.; Lesyk, R. Synthesis of New 4-Thiazolidinone-, Pyrazoline-, and Isatin-Based Conjugates with Promising Antitumor Activity. *J. Med. Chem*. **2012**, 55, 8630-8641. Doi: 10.1021/jm300789g.
10. Barradas, S.; Hernández-Torres, G.; Urbano, A.; Carreño, M.C. Total Synthesis of Natural p-Quinol Cochinchinenone. *Org. Lett.* **2012**, 14, 5952-5955. Doi: 10.1021/ol302858r.
11. Aribert, N.; Camy, S.; Lucchese, Y.P.; Condoret, J.; Cognet, P. Cleaner Routes for Friedel-Crafts Acylation. *Int. J. Chem. React. Eng*. **2010**, 8, 1-13. Doi: 10.2202/1542-6580.2183.
12. Huang, G.; Mo, L.Q.; Wei, Y.X.; Zhou, H.; Guo, Y.A.; Wei, S.J. Effect of Mesoporous Chitosan Action and Coordination on the Catalytic Activity of Mesoporous Chitosan-Grafted Cobalt Tetrakis(p-Sulfophenyl) Porphyrin for Ethylbenzene Oxidation. *Catalysts* **2018**, 8, 1-16. Doi:10.3390/catal8050199.
13. Ricca, C.; Labat, F.; Russo, N.; Adamo, C.; Sicilia, E. Oxidation of Ethylbenzene to Acetophenone with N-Doped Graphene: Insight from Theory. *J. Phys. Chem. C.* **2014**, 118, 12275-12284. Doi: 10.1021/jp502179n.
14. Assal, M.E.; Shaik, M.R.; Kuniyil, M.; Khan, M.; Al-Warthan, A.; Siddiqui, M.R.H.; Adil, S.F. Ag2O Nanoparticles-Doped Manganese Immobilized on Graphene Nanocomposites for Aerial Oxidation of Secondary Alcohols. *Metals* **2018**, 8, 1-22. Doi:10.3390/met8060468.
15. Wei, H.; Liu, K.; Xie, S.; Xin, W.; Li, X.; Liu, S.; Xu, L.; Determination of Different Acid Sites in Beta Zeolite for Anisole Acylation with Acetic Anhydride. *J. Catal.* **2013**, 307, 103-110. Doi: 10.1016/j.cat.2013.07.010.
16. Nakajima, M.; Fukami, H.; Konishi, K.; Oda, J.; Synthesis of Aromatic Carbonyl Compounds by Friedel-Crafts Reaction Using BF_3 Catalyst. *Agric. Biol. Chem.* **1963**, 27, 700-705. Doi: 10.1080/00021369.1963.10858166.
17. Rueping, M.; Nachtsheim, B.J. A review of new developments in the Friedel–Crafts alkylation – From green chemistry to asymmetric catalysis. *Beilstein J. Org. Chem.* **2010**, 6, 1-24. Doi: 10.3762/bjoc.6.6.

18. Halima, T.B.; Zhang, W.; Yalaoui, I.; Hong, X.; Yang, Y.; Houk, K.N.; Newman, S.G. Palladium-Catalyzed Suzuki–Miyaura Coupling of Aryl Esters. *J. Am. Chem. Soc.* **2017**, 139, 1311–1318. Doi: 10.1021/jacs.6b12329.
19. Jiang, Q.; Li, H.; Zhang, X.; Xu, B.; Su, W. Pd-Catalyzed Decarboxylative Sonogashira Reaction via Decarboxylative Bromination. *Org. Lett.* **2018**, 20, 2424–2427. Doi: 10.1021/acs.orglett.8b00772.
20. Mao, J.; Zhang, J.; Zhang, S.; Walsh, P.J. NIXANTPHOS: a highly active ligand for palladium catalyzed Buchwald–Hartwig amination of unactivated aryl chlorides. *Dalton Trans.* **2018**, 47, 8690-8696. Doi: 10.1039/C8DT01852A.
21. Cortés-Borda, D.; Kutonova, K.V.; Jamet, C.; Trusova, M.E.; Zammattio, F.; Truchet, C.; Rodriguez-Zubiri, M.; Felpin, F. Optimizing the Heck–Matsuda Reaction in Flow with a Constraint-Adapted Direct Search Algorithm. *Org. Process Res. Dev.* **2016**, 20, 1979–1987. Doi: 10.1021/acs.oprd.6b00310.
22. Reddy, A.C.S.; Choutipalli, V.S.K.; Ghorai, J.; Subramanian,V.; Anbarasan, P. Stereoselective Palladium-Catalyzed Synthesis of Indolines via Intramolecular Trapping of N-Ylides with Alkenes. *ACS Catal.* **2017**, 7, 6283–6288. Doi: 10.1021/acscatal.7b02072.
23. Wen, C.; Wei, Y.; Tang, D.; Sa, B.; Zhang, T.; Chen, C. Improving the electrocatalytic properties of Pd-based catalyst for direct alcohol fuel cells: effect of solid solution. *Sci. Rep.* **2017**, 7, 1-11. Doi: 10.1038/s41598-017-05323-y.
24. Miranda, R.; Valencia-Vázquez, O.; Maya-Vega, C.A.; Nicolás-Vázquez, I.; Vargas-Rodriguez, Y.M.; Morales-Serna, J.A.; García-Ríos, E.; Salmón, M. Synthesis of Cycloveratrylene Macrocycles and Benzyl Oligomers Catalysed by Bentonite under Microwave/Infrared and Solvent-Free Conditions. *Molecules* **2013**, 18, 12820-12844. Doi: 10.3390/molecules181012820.
25. Salmón, M.; Miranda, R.; Nicolás-Vázquez, I., Vargas-Rodriguez, Y.M.; Cruz-Borbolla, J.; Medrano, M.I.; Morales-Serna, J.A. Effects of Bentonite on p-Methoxybenzyl Acetate: A Theoretical Model for Oligomerization via an Electrophilic-Substitution Mechanism. *Molecules* **2011**, 16, 1761-1775. Doi: 10.3390/molecules16021761.
26. Wahyuningsih, T.D.; Kurniawan, Y.S.; Green Synthesis of Some Novel Dioxolane Compounds from Indonesian Essential Oils as Potential Biogrease. *AIP Conf. Proc.* **2017**, 1823, 020081, Doi: 10.1063/1.4978154.
27. Kurniawan, Y.S.; Ramanda, Y.; Thomas, K.; Hendra; Wahyuningsih, T.D.; Synthesis of 1,4-Dioxaspiro[4.4] and 1,4-Dioxaspiro[4.5] Novel Compounds from Oleic Acid as Potential Biolubricant. *Indones. J. Chem.* **2017**, 17, 301-308. Doi: 10.22146/ijc.24891.
28. Kurniawan, Y.S.; Anwar, M.; Wahyuningsih, T.D.; New Lubricant from Used Cooking Oil: Cyclic Ketal of Ethyl 9,10-Dihidroxyoctadecanoate. *Mater. Sci. Forum* **2017**, 901, 135-141. Doi: 10.4028/www.scientific.net/MSF.901.135.
29. Ghiacia, M.; Sadeghib, Z.; Sedaghata, M.E.; Karimi-Maleha, H.; Safaei-Ghomib, J.; Gil, A. Preparation of Pd (0) and Pd (II) nanotubes and nanoparticles on modified bentonite and their catalytic activity in oxidation of ethyl benzene to acetophenone. *Appl. Catal. A.* **2010**, 381, 121-131. Doi: 10.1016/j.apcata.2010.03.062.
30. Imawan, A.C.; Kurniawan, Y.S.; Lukman, M.F.; Jumina; Triyono; Siswanta, D. Synthesis and Kinetic Study of the Urea Controlled Release Composite Material: Sodium Lignosulfonate from Isolation of Wood Sawdust-Sodium Alginate-Tapioca, *Indones. J. Chem*. **2018**, 18, 108-115. Doi: 10.22146/ijc.26597.
31. Dargóa, G.; Bölcskeib, A.; Grünb, A.; Bénic, S.; Szántód, Z.; Lopatad, A.; Keglevichb, G.; Balogha, G.T. Proton dissociation properties of arylphosphonates: Determination of accurate Hammett equation parameters. *J. Pharm. Biomed. Anal*. **2017**, 143, 101-109. Doi: 10.1016/j.jpba.2017.05.038.
32. Muñoz, H.J.; Blanco, C.; Gil, A.; Vicente, M.Á.; Galeano, L.A.; Preparation of Al/Fe-pillared clays: effect of the starting mineral. *Materials* **2017**, 10, 1364. Doi: 10.3390/ma10121364.
33. Strukul, G.; Lewis Acid Behavior of Cationic Complexes of Palladium(II) and Platinum(II): Some Examples of Catalytic Applications. *Top. Catal.* **2002**, 19, 33-42. Doi: 10.1023/A:1013877131474.
34. Tischler, O.; Kovács, S.; Èrsek, G.; Králl, P.; Daru, J.; Stirling, A.; Novák, Z.; Study of Lewis Acid Accelerated Palladium Catalyzed C-H Activation. *J. Mol. Catal A: Chem.* **2017**, 426B, 444-450. Doi: 10.1016/j.molcata.2016.09.018.
35. Frouri, F.; Célérier, S.; Ayrault, P.; Richard, F.; Inorganic hydroxide fluorides as solid catalysts for acylation of 2-methylfuran by acetic anhydride. *App. Catal. B: Environ.* **2015**, 168-169, 515-523. Doi: 10.1016/j.apcatb.2015.01.020.
36. Crabtree, R.H. *The organometllic chemistry of the transition metals*. **2014**, Wiley, New Jersey.

37. Yamasaki, T.; Makihara, M.; Komura, K.; Zeolite catalyzed highly selective synthesis of 2-methoxy-6-acetylnaphthalene by Friedel-Crafts acylation of 2-methoxynapthalene in acetic acid reaction media. *J. Mol. Catal. A: Chem.* **2017**, 426, 170-176. Doi: 10.1016/j.molcata.2016.11.012.